CELL & GENE THERAPY INSIGHTS

DOWNSTREAM PROCESSING

RESEARCH ARTICLE

Displacement chromatography for enrichment of rAAV genome-containing capsids using weak organic acid

Tamara Zeković, Paul Greback-Clarke, Eric Vorst, Eva Graham, Jordan Hobbs, Robert Tikkanen, Hunter Reese, Amith Naik, Rashmi Bhangale, Carlos Cruz-Teran, Christian Denis, Mayur Jain, Thomas Guarinoni, César Trigueros Fernandez, Jacob Smith, David R Knop, and Joshua C Grieger

Separation of empty and genome-containing particles is a challenging requirement for recombinant adeno-associated virus gene therapy vectors. Strong anion exchange chromatography operated with a linear salt concentration gradient to achieve a high degree of resolution has emerged as the replacement for traditional density-gradient ultracentrifugation to improve efficiency, consistency, and scalability. Herein, an innovative mechanism of anion exchange chromatography using weak organic acid present in the load is shown to selectively displace empty capsids into the flowthrough, enabling an isocratic elution and eliminating operational challenges associated with linear gradients. This separation technique was applied to AAV2 and AAV8 serotypes using three chromatographic media (monoliths, resin, and membranes) and showed comparable genome-containing capsid enrichment levels to that of density gradient ultracentrifugation. Processes for both serotypes were successfully transferred from lab to production scale.

Cell & Gene Therapy Insights 2024; 10(9), 1317–1335

DOI: 10.18609/cgti.2024.150

Recombinant adeno-associated viruses (rAAV) have emerged as promising vectors for transferring therapeutic recombinant genes to humans with several new therapies transitioning to commercialization [1,2]. As advances in upstream processing continue to improve rAAV productivity, traditional downstream purification using density gradient ultracentrifugation processing to enrich genome-containing capsids presents a bottleneck in large scale rAAV purifications [3]. Empty capsids that do not contain the therapeutic gene are an inevitable by-product of the rAAV vector production process and can result in clinical safety and dosage impediments [4,5]. Historically, cesium chloride, sucrose, or iodixanol-based density gradient ultracentrifugation methods have been utilized to separate genome-containing and empty capsids in a serotype-independent manner based on differences in density, as shown in Figure 1. These manual processes are operationally complex at large scale and could result in altering quality attributes important for product and process validations [6–8].

Highly similar size, charge, and accessible surface morphology between the empty and genome-containing capsids makes chromatographic separation of empty capsids challenging for downstream processing of rAAV gene therapy products [9–12]. Ion exchange chromatography has commonly been used in the manufacture of biotherapeutics and the purification of rAAV vectors. Separation of empty from genome-containing capsids has been demonstrated using different modalities of anion exchange (AEX) chromatography such as conventional quaternary amine ligands on resins, monolithic media, and membranes [5,6,13,14]. However, these chromatographic methods primarily use bind and elute strategies with linear salt concentration gradients to resolve impurities like empty capsids [14–16]. A gradient elution strategy can be challenging to implement at commercial scale [17]. Recent developments have shown progress toward a step elution process, but would require minimizing the variation in buffer conductivity, pH, and component additions to achieve a manufacturing ready procedure [13,18–20]. A step elution method capable of separating empty and full capsids in a robust and scalable manner is thus desirable, ensuring consistent product quality between manufacturing batches is attained.

Herein, the AEX load was modified with specific concentrations of a weak organic acid to promote separation based on slight differences in capsids charge and hydrophobicity [21]. This combination of interactions can create different binding strengths for empty capsids and charged stationary phase. Addition of weak organic acid with intermediate binding strength enabled preferential displacement of empty capsids and scalable step elution. Ongoing experiments, utilizing modeling approaches, will help gain further insight into the mechanism of separation.

This method was successfully applied to AAV8 and AAV2 serotypes. Multiple AEX chromatographic media were investigated for each serotype. Substrates with larger pore size or open pore structures were chosen to allow accessibility and faster transport of AAV to binding sites inside the pores of the substrate, which may result in a faster flow rate, higher binding capacity and resolution. Enrichment of genome-containing capsids achieved with this method was comparable to that of density gradient ultracentrifugation for vector manufactured at lab (3 L), pilot (50 L), and production scales (250 L or 500 L).

MATERIALS AND METHODS

Cell culture and rAAV production

Both AAV2 and AAV8 manufacturing processes were initiated with the thaw of a single vial of the suspension HEK293 Pro10 master cell bank (MCB), in chemically defined medium and were expanded through a series of shake flasks to produce sufficient cells to seed a bioreactor at the 3 L scale, 50 L scale,

FIGURE 1

Process flow diagram for both traditional downstream processes and a scalable downstream process without density gradient ultracentrifugation.

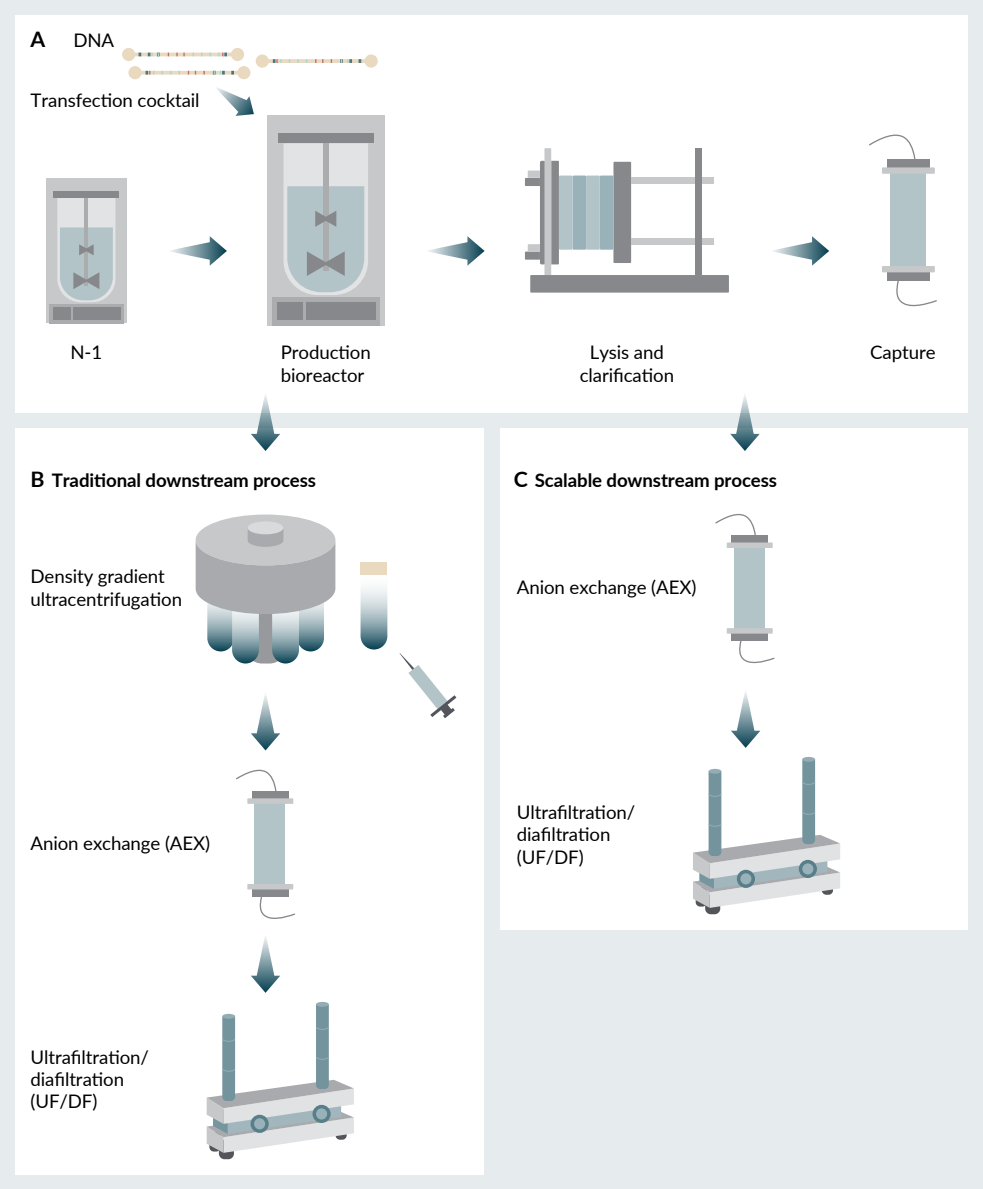

(A) Upstream process, transfection, lysis and clarification, and capture chromatography remains the same for both traditional and scalable processes. **(B)** The traditional process to separate genome-containing capsids from empty capsids includes density gradient ultracentrifugation, AEX to remove the density gradient material such as iodixanol, then UF/DF for buffer exchange. **(C)** A scalable process eliminates the density gradient ultracentrifugation step and uses AEX for separation of genome-containing capsids from empty capsids, then UF/DF for buffer exchange.

or a sequential 50 L and 250 L or 500 L stirring production bioreactor. After expansion of the cells to the target production volume and viable cell density, cells were transfected with a cocktail consisting of adenovirus helper, rep/cap, and transgene-containing neDNA cassette (TAAV Biomanufacturing Solutions, S.L.). Transgene cassettes for AAV8 and AAV2 were single stranded DNA at 4779 kb and 2705 kb lengths, respectively. Cells were harvested approximately 72 hours post-transfection.

Clarification, capture, and anion exchange load preparation

The downstream purification process for both AAV2 and AAV8 was initiated by chemical lysis to release the viral vector from the transfected cells in the bioreactor. Primary clarification was accomplished using 20 µm pore size depth filtration and 0.2 µm sterile filtration. Intact rAAV particles were further purified via capture chromatography using CaptureSelect™ AAVX resin (Thermo Fisher). The affinity-purified eluate was prepared for AEX separation by diluting the product with buffers containing specific amounts of weak organic acids [22]. Buffer compositions were developed to facilitate the interaction between chromatographic media, product, and empty capsids. The load material was filtered through a 0.2 µm filter prior to applying onto the AEX chromatography media.

Density gradient ultracentrifugation

Enrichment of genome-containing capsids was separated by iodixanol gradient ultracentrifugation using a Beckman Ti70 fixed angle rotor. The affinity-purified material was under-layered with 25%, 40% and 60% iodixanol and centrifuged at 505,000 rcf for 1 hour. Genome-containing capsids were extracted from the tube using a syringe at the interface between 40% and 60% iodixanol layers. The iodixanol fractions were pooled and diluted with buffer to reach the desired pH and conductivity required for binding to the AEX media. The genome-containing product was processed over AEX, in a bind-and-elute mode, using a sodium chloride step elution.

Lab scale AEX chromatography

Small-scale AEX chromatographic purifications were performed using 1 mL POROS™ 50HQ prepacked columns (5 cm bed height, Thermo Fisher), 1 mL CIMmultus® QA (2 µm) monolith devices (BIA Separations), or 1 mL Mustang™ Q (Cytiva) membrane devices. Each AEX chromatographic media was evaluated using the same methods, buffers, and load material. Residence times were 1.5 minutes for POROS 50HQ resin, 0.2 minutes for CIMmultus QA monolith, and 0.29 minutes for Mustang Q membrane. Chromatography was performed and 0.25 CV fractions automatically collected by an AKTA Avant™ 25 skid (Cytiva). AKTA skid cleaning in place (CIP) method was performed using 0.5 M sodium hydroxide before each cycle and stored in 20% ethanol.

Initial development of the AEX method included screening different buffer components in the AEX load and gradient elution phase. AEX load was prepared by diluting the affinity eluate with a pH 9.0 buffer containing varying amounts of weak organic acid. Conductivities during the weak organic acid concentration screen ranged from 2.022–2.450 mS/cm for the AAV8 serotype (2.4 mM–6.4 mM weak organic acid) and from 2.276–2.725 mS/cm for the AAV2 serotype (6.4–11.2 mM). The AEX column was equilibrated with the pH 9.0 buffer excluding weak organic acid. Following buffer selections, a 20 CV gradient elution was converted to a step elution, keeping the same buffer components as developed in the gradient elution. During initial development runs, AEX elutions at pH 9.0 were titrated to a neutral pH prior to sample storage and analysis.

AEX purification scale up

At the 3 L scale, the final AEX process for enriching genome-containing capsids utilized POROS 50HQ resin (5 mL, 10 cm bed height) or CIMmultus QA monolith devices (8 mL). POROS 50HQ resin was operated at a 1.5 minute residence time while CIMmultus QA monolith flow rate was at a 1.4 minute residence time to accommodate scaleup requirements.

FIGURE 2

Chromatogram of 20 CV elution gradient using the same prepared AAV8 load over CIMmultus QA monolith, POROS 50HQ resin, and Mustang Q membrane.

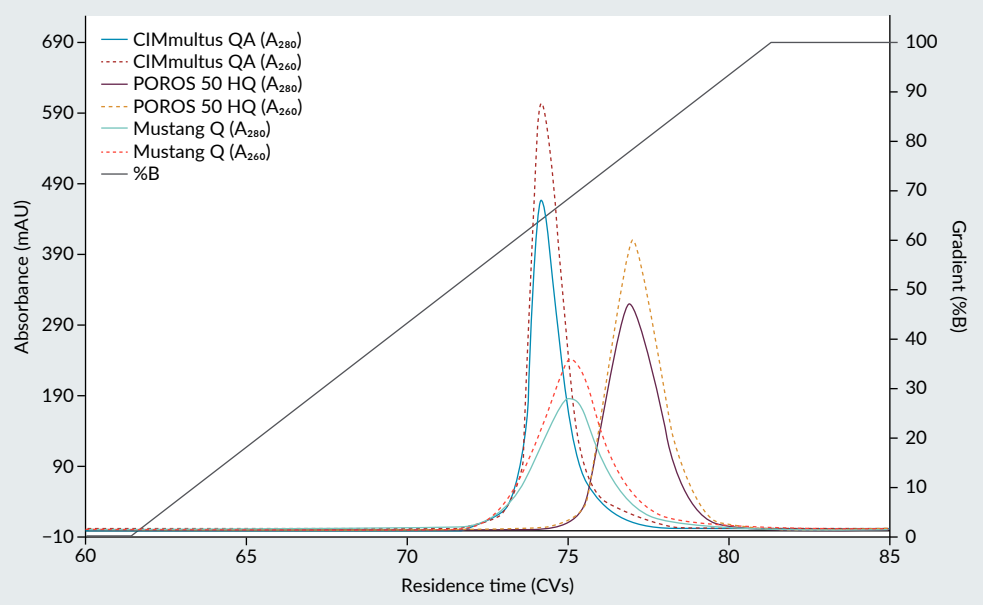

AAV8 was produced at a 50 L pilot scale and a 500 L production scale. An 80 mL CIMmultus QA (2 µm) monolith device was used for 50 L pilot production, and an 800 mL device was used at the 500 L scale on an AKTA Process chromatography skid (Cytiva). AAV2 produced at a 50 L pilot scale used 196 mL (10 cm bed height) POROS 50HQ column, while 250 L production scale used 1.5 L (10 cm bed height) column on an AKTA Process™ chromatography skid (Cytiva).

Elutions during scale up runs were already at a neutral pH and did not require any additional adjustments.

Analytical methods

Viral particle (vp) titers were assessed using an Agilent 1260 Prime II HPLC system (Agilent, Sata Clara, CA) with Agilent Bio SEC-5 4.6 × 150 mm, 500 Å column (Agilent, Santa Clara, CA) to perform size exclusion high performance liquid chromatography (SEC-HPLC). A DAD detector was used to collect traces at 214, 260, and 280 nm. Analysis was performed using Waters® Empower™ 3 software. Viral particle (vp) titers were determined via qualified SEC-HPLC method by integrating the 214 nm peaks and comparing peaks against a standard curve. Standard curves were generated using purified AAV8 or AAV2 for their respective products. The standards had been previously titered by ELISA. Titers generated by SEC-HPLC were used to determine particle recoveries. SEC A_{260}/A_{280} ratios were generated using integrated peak data to provide an estimate of purity for samples not analyzed by analytical ultracentrifugation. All scale up run analyses were performed with qualified SEC-HPLC methods.

Vector genome (vg) titers were assessed with quantitative real time PCR (qPCR) using QuantStudio™ Flex 6 (Thermo Fisher) to determine step recoveries. Custom primers and probes (IDT, Coralville, IA) targeted the ITR region. The forward primer sequence was 5′-GGAACCCCTAGTGATGGAGTT-3′, and the reverse primer sequence was 5′-CGGCCTCAGTGAGCGA-3′. TaqMan™ Fast Advanced Master Mix (Thermo Fisher) facilitated the PCR reaction performed in the thermocycler. The

FIGURE 3

(A) Empty and genome-containing AAV8 capsid distribution in the product (elution pool) by fraction and media type. (B) Recovery of vp and vg in the product (elution pool) by fraction and media type. (C) A260/A280 ratios by both fraction and media type.

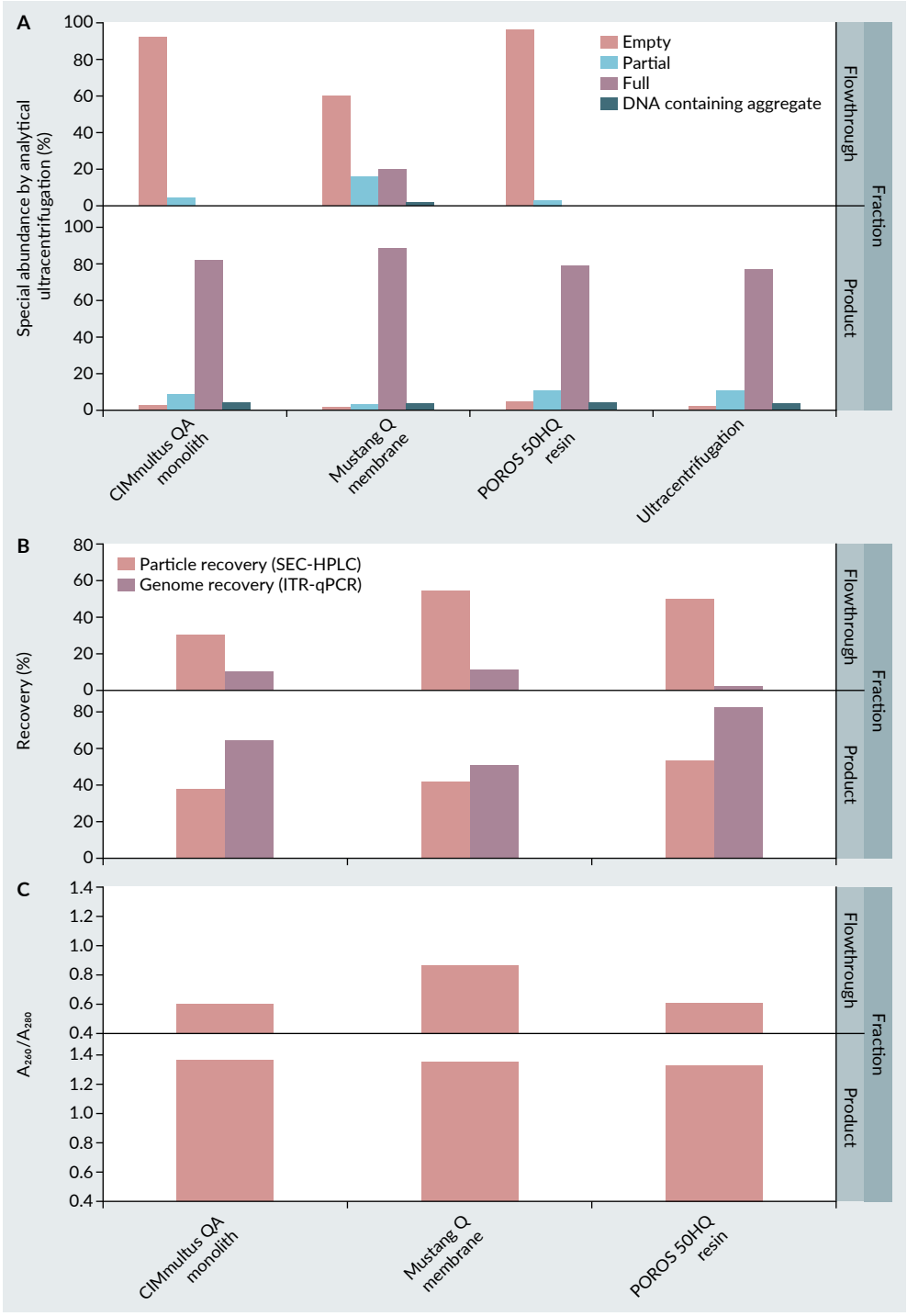

TaqMan probe sequence was 5′-/56-FAM/CACTCCCTCTCTGCGCGCTCG/3BHQ_1/-3.

Qualified ITR-ddPCR was performed for large scale runs using QX200 Droplet Digital™ PCR (ddPCR) system (BioRad, Hercules,

FIGURE 4

Separation of empty and genome-containing AAV8 capsids was modulated by addition of a weak organic acid into the load.

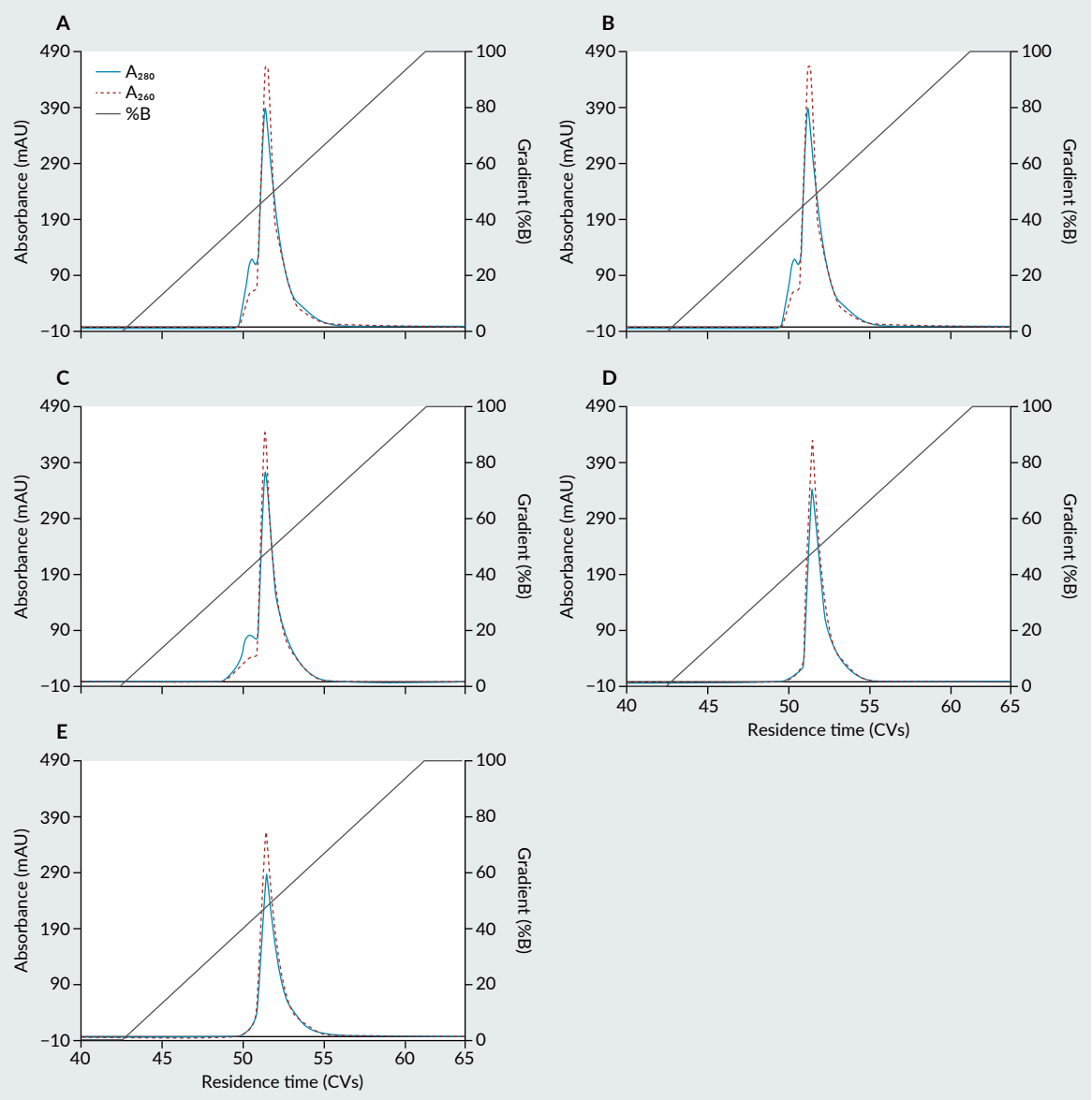

Elution peak chromatograms are shown for loads containing **(A)** 0 mM weak organic acid, **(B)** 2.4 mM weak organic acid, **(C)** 4.0 mM weak organic acid, **(D)** 5.6 mM weak organic acid, and **(E)** 6.4 mM weak organic acid.

CA). Custom, proprietary primers and probes (IDT, Coralville, IA) and TaqMan Fast Advanced Master Mix (Thermo Fisher) were used to perform PCR on droplet samples using a C100 thermocycler (BioRad, Hercules, CA). The QX200 Droplet Reader was then used to detect PCR products and analyzed using QuantaSoft™ RE software (BioRad, Hercules, CA). Trends in recovery were comparable between qPCR and ddPCR assays.

Sedimentation velocity analytical ultracentrifugation (SV-AUC) was analyzed by KBI Biopharma. SV-AUC is a first-principles hydrodynamic technique that determines macromolecular size and conformation directly from a sample in solution. This method is used to assess the viral size distribution and analyze capsid content through the difference in buoyant density between empty and genome-containing capsids. Due

FIGURE 5

Recovery of AAV8 vg by ITR-qPCR and vp by SEC-HPLC titer of pooled fractions with genome-containing capsid enrichment above a SEC A_{260}/A_{280} ratio by SEC-HPLC of 1.20.

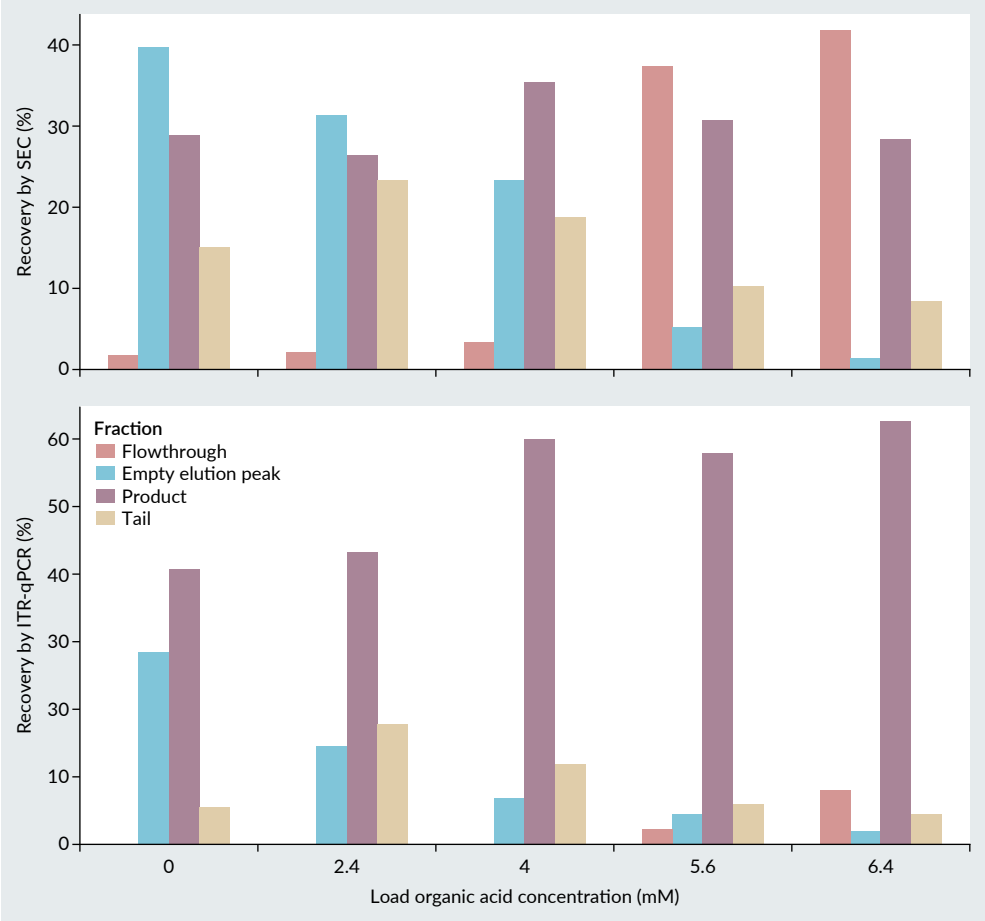

to a greater buoyant density, genome-containing capsids sediment more quickly through solution, compared to empty capsids. Capsids sedimentation is accomplished through centrifugation at high angular velocity. The concentration of each capsid distribution is measured as a function of time and radial position using absorbance optics, and then the concentration profiles can be analyzed to provide information about the different capsid size distribution, plotted as a c(s) distribution. The method works by measuring how much of a particular capsid content is present in a sample, by modeling the expected rates of sedimentation and the rates of diffusion. Each peak in the c(s) distribution is integrated and its area (as a percentage of the total area) represents the relative amount of empty, full, and partially packaged rAAV in a sample [23–25].

RESULTS

AEX media screening selection for removal of empty AAV8 capsids via impurity flowthrough chromatographic method

POROS 50HQ resin, CIMmultus QA monolith, and Mustang Q membrane modalities were evaluated for separation of empty from genome-containing AAV8 capsids. AEX starting materials were generated by diluting affinity eluate (composed of 32%–44% genome containing capsids by AUC) with a

FIGURE 6

Chromatogram showing overlay of 3 L, 50 L, and 500 L purification runs for an AAV8 capsid with a CIMmultus QA substrate.

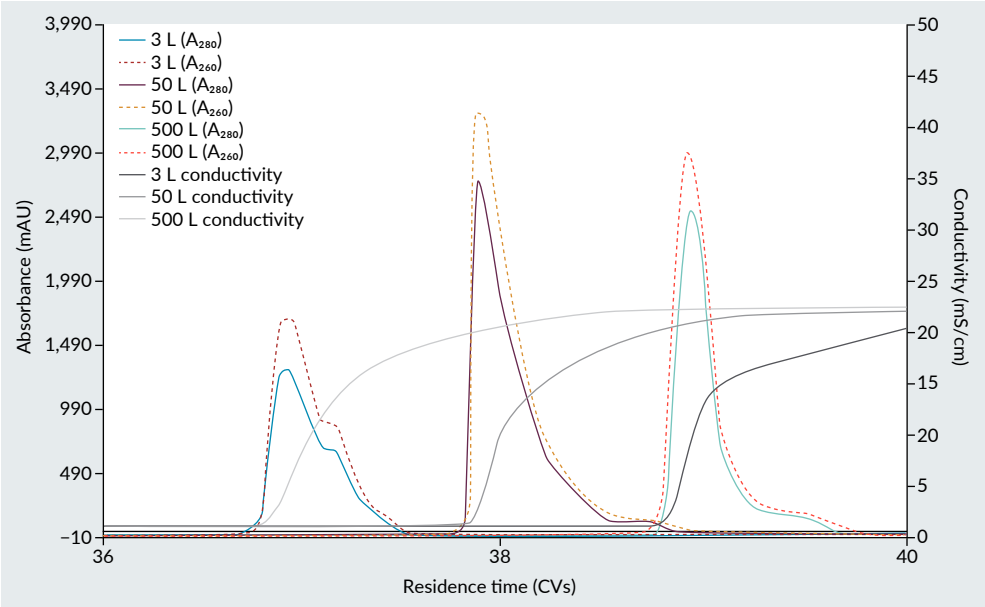

pre-defined concentration of weak organic acid (<10 mM), titrating to pH 9.0, and loading at 2×10^{14} vp per mL of media. As shown in Figure 2, each modality exhibited a similar chromatographic elution profile, indicating genome-containing capsids eluting as single peaks. CIMmultus QA monolith showed the lowest band broadening, followed by POROS 50HQ and Mustang Q membrane. AEX elution fractions from the three modalities were analyzed by SEC-HPLC. Fractions greater than 1.20 by SEC A_{260}/A_{280} were collected to generate the AEX elution pool. The A_{260}/A_{280} ratio from each chromatographic modality elution pool was comparable with the A_{260}/A_{280} ratio of the iodixanol enriched genome-containing capsids.

SV-AUC was used to analyze capsid content through the difference in buoyant density between empty, partial and full capsids. Figure 3A shows equivalent enrichment of full capsids in the AEX elution for the three chromatographic media. Capsid distribution (Figure 3A and C) as well as step recoveries (Figure 3B) were comparable between the chromatography-based and the iodixanol-based gradient enriched full capsids.

Optimization of AAV8 empty and genome-containing capsids separation using CIMmultus QA monolith at lab-scale purification (3 L)

Bioreactors were transfected and processed as shown in Figure 1A. CIMmultus QA monolith was chosen as a chromatographic modality due to the lowest band broadening observed during screening studies, comparable product recovery, and comparable enrichment of genome-containing capsids to iodixanol gradient ultracentrifugation. AEX starting materials were generated by diluting affinity eluate with different concentrations of weak organic acid (0 mM–6.4 mM), titrating to pH 9.0, and loading a 1 mL CIMmultus QA monolith at 2×10^{14} vp per mL of media. A 20 CV linear salt concentration gradient was used to elute the product as shown in Figure 4. Elution profile chromatograms indicated a gradual reduction of empty capsids as the concentration of weak organic acids increased in the AEX load, observed by A_{260}/A_{280} changes in the front half of the elution peak (referred to as empty elution

FIGURE 7

(A) AEX step recoveries (elution pool) of AAV8 by ITR-ddPCR and SEC-HPLC, respectively, for 3 L, 50 L, and 500 L bioreactor using CIMmultus QA monolith. Runs were performed with n=6 for 3 L scale, n=3 for 50 L scale, and n=2 for 500 L scale. Error bars show standard deviation as calculated in JMP. (B) Purity of final product (elution pool) by analytical ultracentrifugation. No 3 L bioreactors were analyzed by SV-AUC due to sampling requirements.

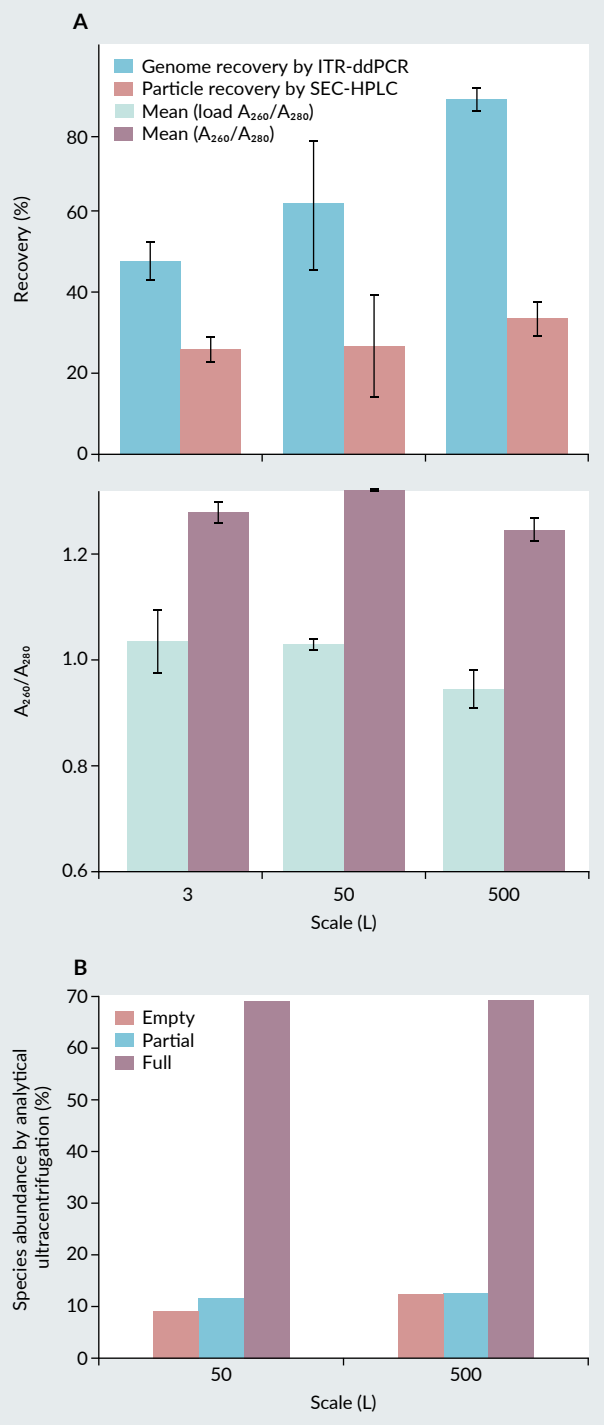

peak). AEX fractions greater than 1.20 by SEC A_{260}/A_{280} were collected to generate the product (AEX elution pool). Post product elution fractions with SEC AA_{260}/A_{280} <1.20 were collected and defined as the tail.

The AEX step recovery was assessed by SEC-HPLC (vector particle recovery), and ITR-qPCR (vector genome recovery) as depicted in Figure 5. The highest reduction of empty capsids and maximized product recovery was achieved for the condition that contained the highest concentration of weak organic acid in the AEX load.

Scaleup of AAV8 empty and genome-containing capsids separation using CIMmultus QA monolith

An isocratic method for AAV8 elution was developed using a CIMmultus QA monolith device after selecting the final concentration of weak organic acid to ensure optimized removal of the empty capsids was achieved during the AEX sample loading phase. Processes that include a step elution are inherently more scalable compared to a linear salt concentration gradient elution due to equipment limitations, buffer mixing from the stationary and mobile phase, and robust product collection criteria. Optimized AEX conditions were evaluated at 3 L, 50 L, and 500 L bioreactor scales, using 8 mL, 80 mL, and 800 mL monolith devices, respectively. Figure 6 shows chromatographic overlay of three comparable elution profiles and consistent enrichment of genome-containing capsids from the 3 L to 500 L purification scale.

AEX step recoveries, assessed by SEC-HPLC for vector particle and ITR-ddPCR for vector genome, were compared across three scales as shown in Figure 7A. CIMmultus QA monolith step recoveries (by ITR-ddPCR) for AAV8 serotype varied from 48% for 3 L scale (n=6) to 89% for 500 L scale (n=2). Genome-containing capsid enrichment, assessed by SV-AUC and SEC A_{260}/A_{280} ratio,

FIGURE 8

Effects of modulating weak organic acid content in the AAV2 load for a CIMmultus QA monolith using a gradient elution method at a concentration of (A) 6.4 mM, (B) 7.2 mM, (C) 8.0 mM, and (D) 8.8 mM.

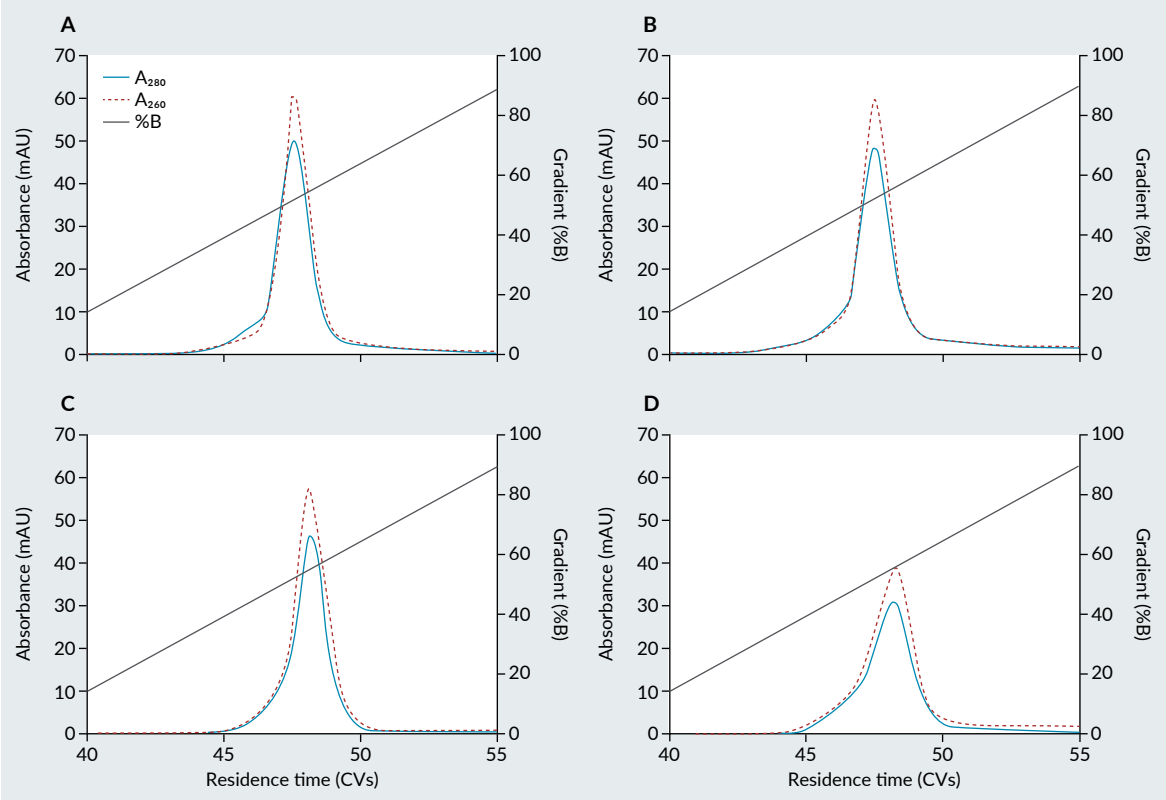

was equivalent between 50 L and 500 L scales as indicated in Figure 7B.

Enrichment of genome-containing AAV2 capsids using POROS 50HQ and CIMmultus QA Monolith

The AEX method developed for enrichment of the AAV8 genome-containing capsids was adapted to an AAV2 vector. Due to differences in charge and hydrophobicity between AAV2 and AAV8 serotypes [21], the AAV2 serotype required modification of the weak organic acid concentration in the AEX load to achieve optimal separation of empty and genome-containing capsids. Three-liter bioreactors were transfected and processed as shown in Figure 1A. AEX starting materials were generated by diluting affinity eluate (composed of 30%–43% genome containing capsids by AUC) with different concentrations of weak organic acid (6.4 mM–11.2 mM), titrating to pH 9.0, and loading on a 1 mL POROS 50HQ or a 1 mL CIMmultus QA monolith at 6×10^{13} vp per mL of media. A 20 CV linear salt concentration gradient was used to elute the product from the CIMmultus QA monolith (Figure 8) and POROS 50HQ (Figure 9). Elution profile chromatograms indicated a gradual reduction of empty capsids as the concentration of weak organic acids increased in the AEX load, observed by A_{260}/A_{280} changes in the front half of the elution peaks.

AEX step recoveries, assessed by SEC-HPLC for vector particle and ITR-qPCR for vector genome, are shown in Figure 10 for CIMmultus QA Monolith and in Figure 11 for POROS 50HQ. AEX fractions greater than 1.20 by SEC A_{260}/A_{280} were collected to generate the AEX elution pool. The highest product recovery was achieved for the condition containing 6.5 mM concentration of weak organic acid in the AEX load

FIGURE 9

Gradient elution profile for increasing concentration of the weak organic acid in the AAV2 load of POROS 50HQ from (A) 8.8 mM, (B) 9.6 mM, (C) 10.4 mM, to (D) 11.2 mM.

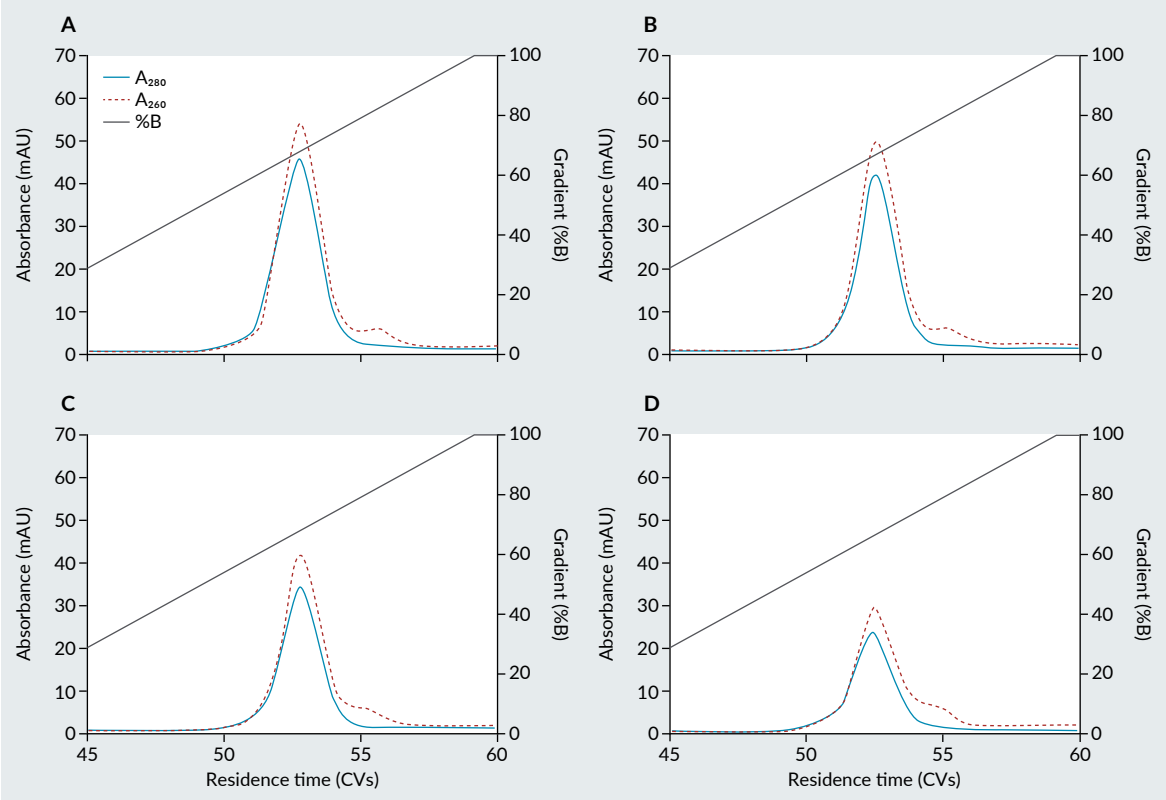

for CIMmultus QA monolith or 9.5 mM concentration for POROS 50HQ. Due to slightly higher product recovery and comparable enrichment by SEC A_{260}/A_{280} achieved with POROS 50HQ, this resin was selected for scale up to 50 L and 250 L bioreactors.

Scaleup of AAV2 empty and genome-containing capsids separation using POROS 50HQ

Prior to AAV2 POROS 50HQ scaling, a 20 CV linear salt elution gradient was converted to isocratic step elution by selecting an optimal elution conductivity to minimize operational challenges at the large manufacturing process. Isocratic step elution was performed at the 3 L, 50 L, and 250 L scales, using 5 mL, 200 mL, and 1500 mL POROS 50HQ columns, respectively. The 250 L purification was performed using an oversized column to match operational parameters and be within the loading specifications at 500 L manufacturing scale. Comparable elution profile chromatograms for all three scales are shown in Figure 12.

Comparable recoveries by SEC-HPLC and ITR-ddPCR across three scales are presented in Figure 13A. Greater than 70% AEX step recovery by ITR-ddPCR was conserved between the 3 L and 250 L scale. Large scale runs, 50 L and 250 L, were analyzed for capsids distribution using SV-AUC as shown in Figure 13B. Greater than 80% genome-containing AAV2 capsid enrichments were achieved across all scales with less than 6% high and low molecular mass species content.

DISCUSSION

Experimental results collectively led to successful separation of empty and genome-containing capsids for both AAV8 and AAV2 serotypes. Weak organic acid present in the

FIGURE 10

AEX step recoveries (elution pool) of particle capsids and genome-containing capsids by SEC-HPLC and ITR-qPCR and A260/A280 by SEC-HPLC for the CIMmultus QA monolith modality.

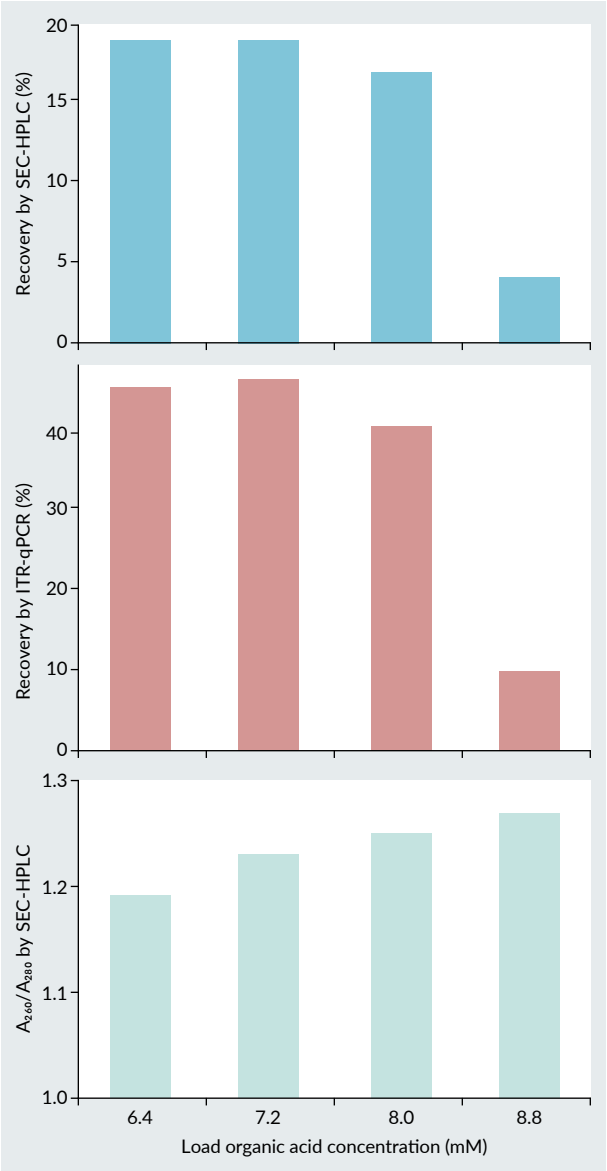

FIGURE 11

Recoveries of total capsids and genome-containing capsids by SEC-HPLC and ITR-qPCR and A260/A280 by SEC-HPLC for the POROS 50HQ resin modality.

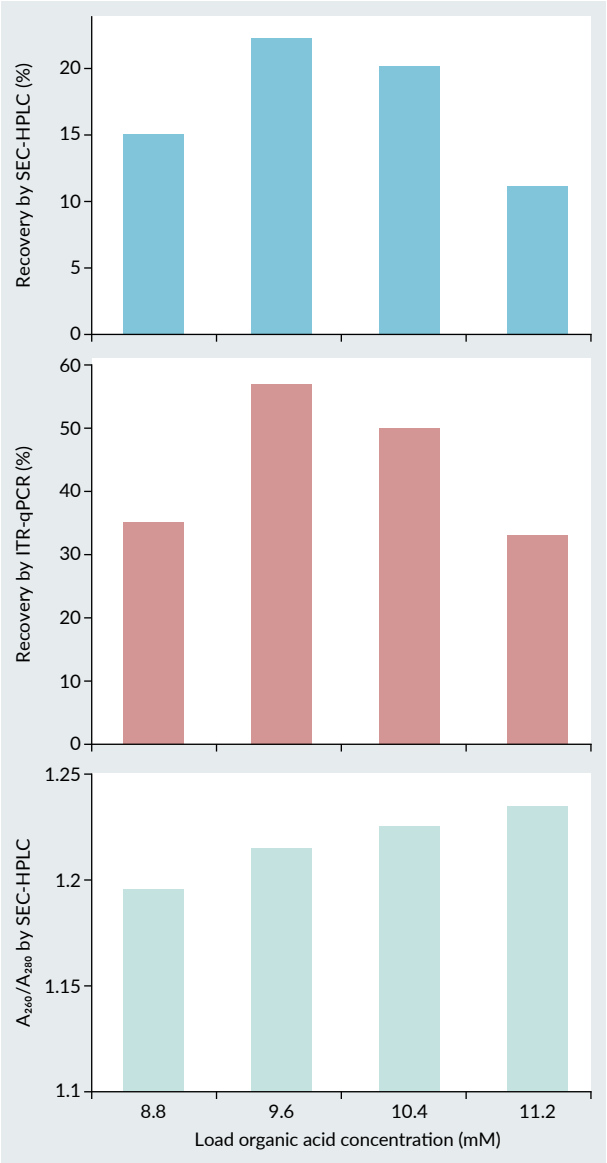

AEX load excluded empty capsids from binding to the media and provided sufficient resolution for chromatographic capsids separation. The hypothesis of the mechanism is that, as the load material is applied to the media, only empty capsids are selectively displaced by weak organic acid due to its higher affinity to the positively charged anion exchange groups. Data from Figure 5 supported the separation was driven by changes in the concentration of weak organic acids and not by changes in conductivity. Increasing concentration of weak organic acid from 2.4 mM–6.4 mM for AAV8 serotype raised the conductivity of the load from 2.022–2.450 mS/cm, and increasing the weak organic acid concentration 6.4 mM–11.2 mM for AAV2 serotype raised the conductivity of the load from 2.276–2.725 mS/cm. These small conductivity differences between increased

FIGURE 12

Chromatogram showing overlay of 3 L, 50 L, and 250 L purification runs for an AAV2 capsid using POROS 50HQ resin.

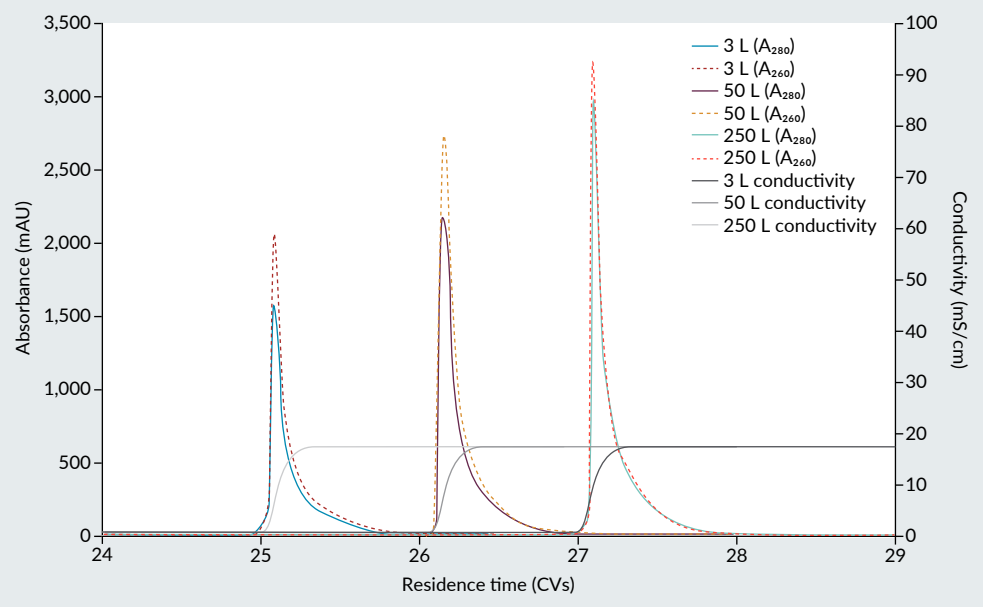

concentration of weak organic acid are unlikely to be the determinative factor in binding selectivity. Further studies are ongoing to understand the mechanism of separation by utilizing modeling approaches.

AAV8 development and scaleup

As shown in the elution chromatograms in Figure 4, increased weak organic acid concentration diminished the early-eluting empty capsid peak during the 20 CV gradient elution. The reduction of front shoulder peak intensity indicated the concentration of weak organic acid in the load was inversely proportional to the amount of empty capsids in the eluate fractions, as shown by SEC-HPLC analysis. The recovery of genome-containing product by ITR-qPCR also increased as the weak organic acid in the load improved resolution between empty and genome-containing capsids. An optimal concentration of weak organic acid was identified by monitoring the loss of genome-containing capsids in the flowthrough fraction and maximizing capsid enrichment. These results confirmed tuning the concentration of weak organic acid in the load was an effective method to achieve empty and genome-containing capsid separation by displacing the empty capsids into the flowthrough during loading of the AEX column.

Mustang Q membrane showed the lowest recovery during the initial modality screening and was not selected for scale up of AAV2 or AAV8 serotype. Lower step recovery could be due to unoptimized processing parameters or peak broadening, which is observed with membrane geometries [26,27]. However, by modulating the weak organic acid in the AEX load (Figures 5, 10, and 11), the ratio of empty and genome-containing capsids could be tunable for all modalities tested, including Mustang Q membrane. As shown in Figure 2, CIMmultus QA monolith provided a higher resolution and comparable step recovery for AAV8 compared to POROS 50HQ. It was selected for further development of AAV8 empty and genome-containing capsids.

The AAV8 serotype was scaled from 3 L to 50 L pilot and 500 L production process. As shown in Figure 6, the chromatographic elution peaks showed similar shape at all three scales. The 3 L runs were performed at a challenge of

3.2×10^{13} vp per mL of media, while 50 L and 500 L runs were performed at 1.0×10^{14} and 7.2×10^{13} vp per mL of media, respectively. However, lower challenge at the 3 L scale did not affect the chromatographic separation and enrichment of genome-containing capsids.

CIMmultus QA monolith step recoveries (by ITR-ddPCR) for AAV8 serotype varied from 48% for 3 L scale (n=6) to 89% for 500 L scale (n=2). This variability may be caused by column loading challenge differences or higher product loss during sampling. Additionally, work with monoliths (data not shown) appeared to demonstrate lot-to-lot variability which may explain some of the difference across various scales of CIMmultus QA monolith, and recent monolith developments may address this variability [28]. As shown in Figure 7, chromatographic separation could effectively remove empty capsids and achieve comparable distribution of empty and genome-containing capsids compared to traditional separation using density gradient ultracentrifugation. This demonstrated the scalability of the AEX method which included the use of weak organic acid to displace the empty capsids into the flowthrough while selectively binding genome-containing capsids.

Adapting AAV8 process to an AAV2 serotype

With an AAV2 product, both CIMmultus QA monolith and POROS 50HQ resin AEX modalities demonstrated separation of empty and genome-containing capsids under the conditions explored. The two modalities showed adjusting the concentration of organic acid in the load could be a suitable approach to improve separation of empty and genome-containing capsids. Due to the higher product recovery provided by POROS 50HQ resin (CIMmultus QA monolith results in Figure 10 and POROS 50HQ resin results in Figure 11) during the initial media screen, this modality was selected for further refinement of weak acids in the AEX load and scaled to a

FIGURE 13

(A) Recoveries of different particle species for 3 L, 50 L, and 250 L bioreactor scale AEX purifications of an AAV2 capsid with POROS 50HQ resin. Runs were performed with an n=1. (B) Analytical centrifugation results for AEX eluates of 50 and 250 L scale runs.

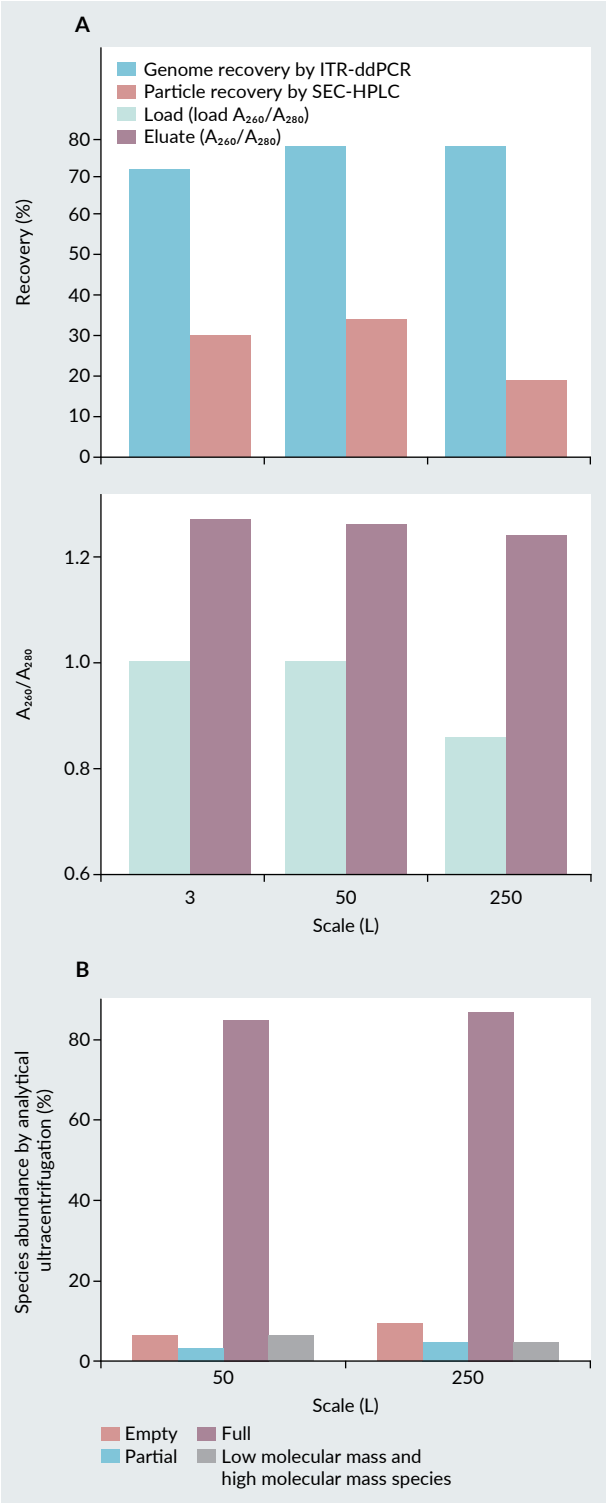

250 L bioreactor. Both the pilot and the production POROS 50HQ run showed comparable elution chromatograms (Figure 12), AEX step recoveries (Figure 13A) and enrichment of genome-containing capsids (Figure 13B). The vector genome (ITR-ddPCR) AEX step recovery varied from 71% for 250 L to 78% for 50 L bioreactor scale. Enrichment of genome-containing capsids was measured by SV-AUC and was consistently above 80%, ranging from 85% for the 50 L scale to 87% for the 250 L scale. This was comparable to the 89% genome-containing capsids achieved by traditional iodixanol density gradient ultracentrifugation preparation. This successful development and scalability mimicked the approach and purification results shown by the AAV8 AEX process.

CONCLUSION

The addition of weak organic acid during AEX load preparation led to a scalable, robust separation of empty and genome-containing capsids. Sufficient removal of the empty capsids into the AEX flowthrough fraction was induced without causing early product release of the genome-containing AAV2 or AAV8 serotype. Selective binding of the genome-containing capsids allowed elution in a stepwise manner while achieving a high AEX step recovery and capsid enrichment. Product enrichment was accomplished across different chromatographic media and scaled to 250 L (AAV2) or 500 L (AAV8) by modulating weak organic acid concentration in the AEX load. AAV8 serotype was enriched from 25%–65% genome containing capsids, while AAV2 serotype was enriched from 40%–80% genome containing capsid. This chromatographic method was successfully converted from linear to step elution and scaled for two serotypes to achieve comparable level of separation to that obtained with iodixanol density gradient ultracentrifugation. This innovative AEX method can serve as a scalable platform approach for separation of empty and genome-containing capsids for other rAAV serotypes.

Chromatographic removal of empty capsids during the AEX load and conversion from linear gradient to step elution can significantly simplify the control strategy for large scale manufacturing. This approach offers a robust, scalable, and cost-effective process with possibilities to utilize versatile elution buffers optimized for different rAAV gene therapy products. This advancement in chromatographic displacement for the enrichment of genome-containing rAAV removes the need to use density gradient ultracentrifugation at large manufacturing scales.

TRANSLATIONAL INSIGHT

An isocratic step-elution based chromatography method that elutes genome-containing rAAV from AEX after displacing empty capsids into the AEX flowthrough can be achieved using any chromatographic skid while achieving product quality requirements. The chromatographic displacement technology can be adapted to all current well-established rAAV scalable manufacturing platform processes. This technology will have a significant impact on future high cell density stable rAAV producer cell line manufacturing processes that transition to continuous processing. Improvements in manufacturing process and technologies will ultimately lead to improved yields, quality attributes, efficiencies and lower COGs for rAAV gene therapy vectors for patients with genetic diseases.

REFERENCES

1. Bulcha JT, Wang Y, Ma H, Tai PWL, Gao G. Viral vector platforms within the gene therapy landscape. *Sig. Transduct. Target Ther.* 2021; 6(53), 1–24.

2. Jiang F, Zhang C, Liu W, *et al.* Bibliometric analysis of global research trends in adeno-associated virus vector for gene therapy

(1991–2022). *Front. Cell. Infect. Micribiol.* 2023; 13, 1301915.

3. Escandell JM, Pais DAM, Carvalho SB, *et al.* Leveraging rAAV bioprocess understanding and next generation bioanalytics development. *Curr. Op. Biotechnol.* 2022; 74, 271–277.

4. Wright JF. Product-related impurities in clinical-grade recombinant rAAV vectors: characterization and risk assessment. *Biomedicines* 2014; 2(1), 80–97.

5. Wright, JF. rAAV vector manufacturing process design and scalability—bending the trajectory to address vector-associated immunotoxicities. *Mol. Ther.* 2022; 30(6), 2119–2121.

6. Hebben M. Downstream bioprocessing of rAAV vectors: industrial challenges and regulatory requirements. *Cell & Gene Therapy Insights* 2018; 4(2), 131–146.

7. Wada M, Uchida N, Posadas-Herrera G, *et al.* Large-scale purification of functional rAAV particles packaging the full genome using short-term ultracentrifugation with a zonal rotor. *Nat. Gene Ther.* 2023; 30, 641–648.

8. Grieger JC, Soltys SM, Samulski RJ. Production of recombinant adeno-associated virus vectors using suspension HEK293 cells and continuous harvest of vector from the culture media for GMP FIX and FLT1 clinical vector. *Mol. Ther.* 2016; 24(2), 287–297.

9. Srivastava A, Mallela KMG, Deorkar N, Brophy G. Manufacturing challenges and rational formulation development for rAAV viral vectors. *J. Pharm. Sci.* 2021; 110(7), 2609–2624.

10. Smith J, Grieger J, Samulski J. Overcoming bottlenecks in rAAV manufacturing for gene therapy. *Cell & Gene Therapy Insights* 2018; 4(8), 815–827.

11. Wang C, Mulagapati SHR, Chen Z, *et al.* Developing an anion exchange chromatography assay for determining empty and full capsid contents in AAV6.2. *Mol. Ther. Methods Clin. Dev.* 2019; 15, 257–263.

12. Qu G, Bahr-Davidson J, Prado J, *et al.* Separation of adeno-associated virus type 2 empty particles from genome containing vectors by anion-exchange chromatography. *J. Virological Meth.* 2006; 140, 183–192.

13. Joshi PRH, Bernier A, Moco PD, Schrag J, Chahal PS, Kamen A. Development of a scalable and robust AEX method for enriched rAAV preparations in genome-containing VCs of serotypes 5, 6, 8, and 9. *Mol. Ther. Methods Clin. Dev.* 2021; 21, 341–356.

14. Nass SA, Mattingly MA, Woodcock DA, *et al.* Universal method for the purification of recombinant rAAV vectors of differing serotypes. *Mol. Ther. Methods Clin. Dev.* 2018; 9, 33–46.

15. Qu G, Wright JF. Methods for producing preparations for recombinant rAAV virions substantially free of empty capsids. PCT/US2017/0260545. Genzyme Corporation. Sep 14, 2017.

16. Tomono T, Hirai Y, Okada H, *et al.* Highly efficient ultracentrifugation-free chromatographic purification of recombinant rAAV serotype 9. *Mol. Ther. Methods Clin. Dev.* 2018; 11, 180–190.

17. Gagnon P, Leskovec M, Goricar B, Strancar A. Streamlining industrial purification of adeno-associated virus. *BioProcess International* Dec 17, 2020. https://www.bioprocessintl.com/separation-purification/streamlining-industrial-purification-of-adeno-associated-virus.

18. Aebischer MK, Gizardin-Fredon H, Lardeux H, *et al.* Anion-exchange chromatography at the service of gene therapy: baseline separation of full/empty adeno-associated virus capsids by screening of conditions and

step-gradient elution mode. *Int. J. Mol. Sci.* 2022; 23, 12332.

19. Di W, Koczera K, Zhang P, Chen DP, Warren JC, Huang C. Improved adeno-associated virus empty and full capsid separation using weak partitioning multi-column AEX chromatography. *Biotechnol. J.* 2024; 19(1), 2300245.

20. Dickerson R, Argento C, Pieracci J, Bakhshayeshi M. Separating empty and full recombinant adeno-associated virus particles using isocratic anion exchange chromatography. *Biotechnol. J.* 2021; 16, 2000015.

21. Heldt CL, Areo O, Joshi PU, Mi X, Ivanova Y, Berrill A. Empty and full rAAV capsid charge and hydrophobicity differences measured with single-particle AFM. *Langmuir.* 2023; 39, 5641–5648.

22. Zekovic T, Smith C, Greback-Clarke P, *et al.* Method for purifying recombinant viral particles.PCT/US2022/013279. Asklepios Biopharmaceutical, Inc. Jul 28, 2022.

23. Burnham B, Nass S, Kong E, *et al.* Analytical ultracentrifugation as an approach to characterize recombinant adeno-associated viral vectors. *Hum. Gene Ther. Meth.* 2015; 26(6), 228–242.

24. Maruno T, Ishii K, Torisu T, Uchiyama S. Size distribution analysis of the adeno-associated virus vector by the c(s) analysis of band sedimentation analytical ultracentrifugation with multiwavelength detection. *J. Pharm. Sci.* 2023; 112(4), 937–946.

25. Yarawsky AE, Zai-Rose V, Cunningham HM, Burgner JW, DeLion MT, Paul LN. rAAV analysis by sedimentation velocity analytical ultracentrifugation: beyond empty and full capsids. *Eur. Biophys. J.* 2023; 52(4–5), 353–366.

26. Qu Y, Bekard I, Hunt B, *et al.* The transition from resin chromatography to membrane adsorbers for protein separations at industrial scale. *Sep. Pur. Rev.* 2022; 21(1), 1542–2119.

27. Nath A, Zin MM, Molnar MA, *et al.* Membrane chromatography and fractionation of proteins from whey—a review. *Process* 2022; 10(5), 1025.

28. Aleš Štrancar. New empty/full method to enable robust manufacturing of rAAV products. Webinar *Cell & Gene Therapy Insights* Oct 12, 2023. https://www.insights.bio/cell-and-gene-therapy-insights/webinars/486/New-empty-full-method-to-enable-robust-manufacturing-of-AAV-products.

AFFILIATIONS

Tamara Zeković
Asklepios Bio, Durham, NC, USA
(Author for correspondence)
tzekovic@askbio.com

Paul Greback-Clarke
Asklepios Bio, Durham, NC, USA

Eric Vorst
Asklepios Bio, Durham, NC, USA

Eva Graham
Asklepios Bio, Durham, NC, USA

Jordan Hobbs
Asklepios Bio, Durham, NC, USA

Robert Tikkanen
Asklepios Bio, Durham, NC, USA

Hunter Reese
Asklepios Bio, Durham, NC, USA

Amith Naik
Asklepios Bio, Durham, NC, USA

Rashmi Bhangale
Asklepios Bio, Durham, NC, USA

Carlos Cruz-Teran
Asklepios Bio, Durham, NC, USA

Christian Denis
Asklepios Bio, Durham, NC, USA

Mayur Jain
Asklepios Bio, Durham, NC, USA

Thomas Guarinoni
Viralgen, San Sebastián, Spain

César Trigueros Fernandez
Viralgen, San Sebastián, Spain

Jacob Smith
Asklepios Bio, Durham, NC, USA

David R Knop
Asklepios Bio, Durham, NC, USA

Joshua C Grieger
Asklepios Bio, Durham, NC, USA

AUTHORSHIP & CONFLICT OF INTEREST

Contributions: The named authors take responsibility for the integrity of the work as a whole, and have given their approval for this version to be published.

Acknowledgements: The team would like to acknowledge Process Development and Analytical Development groups at Asklepios Biopharmaceutical, Inc.

Disclosure and potential conflicts of interest: Tamara Zekovic, Paul Greback-Clarke, Eric Vorst, Eva Graham, Jordan Hobbs, Robert Tikkanen, Hunter Reese, Rashmi Bhangale, Carlos Cruz-Teran, Christian Denis, Amith Naik, Jacob Smith, David Knop, and Joshua Grieger are employees of Asklepios Biopharmaceutical, Inc. Tamara Zekovic and Joshua Grieger hold the patent: Method for purifying recombinant viral particles, publication number: 20240084268. Paul Greback-Clarke and Eric Vorst hold patent PCT/US2022/013279. Eva Graham holds patent publication 2022/159679. Jordan Hobbs holds patent WO2022159679. Robert Tikkanen has an AskBio associated patent with this technology (publication number: 20240084268). Thomas Guarinoni is an employee of Viralgen, which was partly involved in this work. Jacob Smith holds patent publication number 20240084268, and received stock options from AskBio, Inc. Joshua Grieger is an equity holder of Asklepios Biopharmaceutical, Inc.

Funding declaration: The work included in this article was funded by AskBio by way of employing the authors.

ARTICLE & COPYRIGHT INFORMATION

Article source: Invited; externally peer reviewed.

Submitted for peer review: Jul 23, 2024; **Revised manuscript received:** Oct 9, 2024;
Publication date: Oct 25, 2024.